Studies of track finding for long-lived particles at STCF*

Hao Li,[1] Hang Zhou,[2,3] Jin Zhang,[4] Xingtao Huang,[5] Jie Yang,[1] and Xiaocong Ai[1,†]

[1]*School of Physics, Zhengzhou University, Zhengzhou 450001, China*
[2]*State Key Laboratory of Particle Detection and Electronics, University of Science and Technology of China, Hefei 230026, China*
[3]*Department of Modern Physics, University of Science and Technology of China, Hefei 230026, China*
[4]*School of Science, Shenzhen Campus of Sun Yat-sen University, Shenzhen 518107, China*
[5]*Institute of Frontier and Interdisciplinary Science, Shandong University, Qingdao 266327, China*

Reconstruction of the trajectories of charged particles at High Energy Physics experiments is a complicated task, in particular those of long-lived particles. At the future Super Tau-Charm Facility (STCF), long-lived particles are present in several important benchmark physics processes. A Common Tracking Software was used to reconstruct the trajectories of long-lived particles and it is shown that the track finding performance of the commonly used Combinatorial Kalman Filter for long-lived particles is limited by the seeding algorithm. This can be improved by steering the Combinatorial Kalman Filter with initial tracks provided by Hough Transform. The track finding performance of combined Hough Transform and Combinatorial Kalman Filter evaluated using the process $J/\psi \to \Lambda(\to p\pi^-)\bar{\Lambda}(\to \bar{p}\pi^+)$ at STCF is presented.

Keywords: Track finding, Common tracking software, Hough Transform, Long-lived particles

I. INTRODUCTION

Standard Model (SM) [1, 2] of particle physics including the unified Electro-Weak (EW) and Quantum Chromo-Dynamics (QCD) theories, has explained successfully almost all experimental results about the microscopic world. However, a couple of questions still remain, e.g. baryon asymmetry of the universe, dark matter, neutrino masses, number of flavors. Beijing Electron Positron Collider (BEPCII) - Beijing Spectrometer (BESIII) [3] is the only multi-GeV e^+e^- collider operating in the τ-charm sector, which provides an unique platform for studying non-perturbative QCD and strong interactions of the SM. The Super Tau-Charm Facility (STCF) [4, 5] is designed to continue and extend the physics programs at BEPCII in near future, including probing the nature of the strong interactions and hadron structure, precise inspection of electroweak theories, exploring the asymmetry of matter-antimatter and searching for new physics beyond the SM. STCF will operate at a center-of-mass-energy of 2-7 GeV and a peak luminosity above 0.5×10^{35} cm^{-2} s^{-1}, which is two orders higher than that at BEPCII.

The reconstruction of charged particles is the most fundamental and critical step in the data processing chain of High Energy Physics (HEP) experiments. To fulfill the physics goals and to further maximize the physics potential at the STCF, the charged particles need to be reconstructed with good efficiency. This includes not only those particles that decay immediately upon production but also the long-lived particles [6], e.g. the Λ and Ξ hyperons, which are relevant with a couple of important physics goals at STCF. For example, the weak decays of the Λ and Ξ hyperons provide promising channels for searching for new sources of CP violation [7–9]. The hyperon samples at STCF can also be used to measure the time-like nucleon and hyperon form factors for Q^2 values as high as 40 GeV^2 [5]. Meanwhile, it is quite challenging to reconstruct the trajectories of long-lived particle decay products because the long-lived particles may decay within or outside the inner tracker hence having very limited number of hits recorded by the inner tracker.

The Kalman Filter (KF) [10] algorithm is the most commonly used algorithm for tracking in HEP and nuclear physics. The Combinatorial Kalman Filter (CKF) [11, 12] is an extended version of the KF, where the measurements are progressively added to the track during the track propagation steered by an initial estimate of the track parameters, i.e. seed. The impact of magnetic field and material effects is incorporated during track propagation hence CKF is capable to resolve the hit ambiguity in a very dense tracking environment. For this reason, CKF is deployed to find tracks by several experiments e.g. ATLAS [13] and CMS [14], where thousands of tracks are present in a single event. CKF is also the primary track finding algorithm at BelleII experiment [15]. Recently, the CKF algorithm developed by BelleII experiment was reused to study the tracking performance [16] at the Circular Electron-Positron Collider (CEPC) [17]. Despite the great advantages of CKF, one downside of the KF-based tracking algorithms is that they are subject to the performance of the seeding algorithm, which might provide poor performance for long-lived particles. Recently, a track finding algorithm based on the Hough Transform used by BelleII experiment [18] and BESIII experiment [19] has been developed at STCF [20], where tracking performance for prompt particles without vertex displacement have been studied. It demonstrates promising tracking performance, in particular good robustness against local hit inefficiency. However, the tracking efficiency can be deteriorated by the presence of background hits at low transverse momentum.

The ACTS (A Common Tracking Software) [21, 22] is an emerging open-source tracking software for HEP and nuclear physics experiments, with a suite of detector-agnostic and framework-independent modular track and vertex reconstruc-

* Supported by the National Natural Science Foundation of China (Nos. 12375194, 12341504, 12375197, 12025502)

† Corresponding author, xiaocongai@zzu.edu.cn

tion algorithms. The promising performance of the KF and CKF algorithms in ACTS is underscored by their widespread adoption by experiments such as FASER [23], sPHENIX [24] and a few R&D studies at STCF [25] and BESIII [26]. Notably, ACTS has demonstrated its generality across a series of tracking detector types [27]. However, the performance of ACTS for long-lived particles has not been investigated.

In this study, the tracking performance of STCF with a fully gaseous tracking system consisting of a μ-RWELL [28]-based inner tracker and a drift chamber using combined Hough Transform and ACTS CKF to boost the tracking performance for long-lived particles is studied. The manuscript is organized as follows. Section II presents a brief introduction of the STCF detector. In Section III, the tracking workflow with different algorithms is introduced. Section IV focuses on tracking performance for benchmark process with long-lived particles at STCF. A brief conclusion is given in Section V.

II. STCF DETECTOR

The STCF detector [5] ensures comprehensive coverage of the solid angle encompassing the collision point, as depicted in Fig. 1. The STCF detector consists of a tracking system comprising an Inner Tracker (ITK) and a Main Drift Chamber (MDC), along with a Ring Imaging Cherenkov (RICH) detector [29] and a DIRC-like Time-of-Flight (DTOF) detector [30] for particle identification in the barrel and endcap regions. Additionally, it incorporates a uniform Electro-magnetic Calorimeter (EMC) [31], a superconducting solenoid magnet generating 1 Tesla axial magnetic field, and a Muon Detector (MUD) positioned at the detector system's outermost layer.

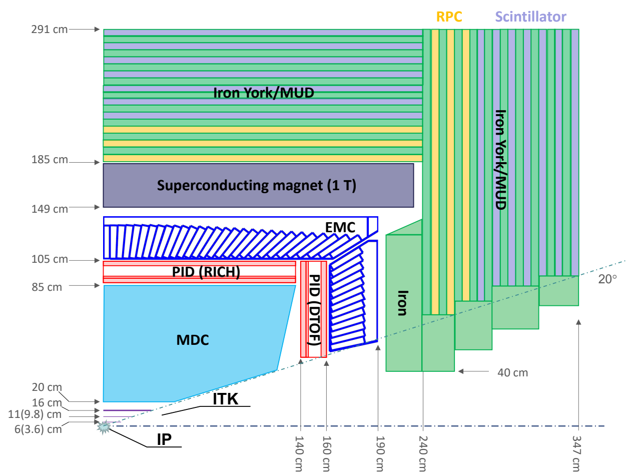

Fig. 1. Schematic layout of the STCF detector. The number in brackets indicate the radii of the MAPS-based ITK. Figure is taken from Ref. [5].

To ensure optimal tracking efficiency for low-momentum charged particles, the ITK within the tracking system covering a polar angle range of 20° to 160° (i.e. $|\cos\theta| < 0.94$) comprises three layers of low-material budget silicon or gaseous detectors using either MAPS-based or μ-RWELL-based technology [28]. This study focuses on the μ-RWELL-based ITK with the three layers placed at an inner radii of 60 mm, 110 mm, and 160 mm, respectively, and each layer has a thickness of approximately 6.5 mm. It provides a spatial resolution around 100 μm in the r-ϕ direction and around 400 μm in the z direction. For the MAPS-based ITK, the radii of the three silicon layers is 36 mm, 98 mm and 160 mm, respectively, and a hit resolution of 30 μm $\times$ 180 μm is assumed. Unless explicitly specified, ITK denotes the μ-RWELL-based ITK by default.

Central to the tracking system of the STCF detector, the Main Drift Chamber (MDC) operates using a He/C_3H_8(60/40) gas mixture and features a square cell configuration with a superlayer wire arrangement. The superlayers within the MDC alternate between stereo layers ("U" or "V") and axial layers, each containing six layers. In total, the MDC comprises eight superlayers (AUVAUVAA) and 48 layers, with inner and outer radii of 200 mm and 850 mm, respectively. The MDC provides spatial resolutions ranging between 120 μm and 130 μm.

III. TRACK RECONSTRUCTION USING COMBINED HOUGH TRANSFORM AND CKF

The workflow of track reconstruction using combined Hough Transform and ACTS CKF is illustrated in Fig. 2. The ACTS CKF is used to find track candidates through track fitting steered by the initial track parameters provided by either ACTS seeding algorithm or Hough Transform algorithm developed within the STCF offline software.

A. Interface between STCF offline software and ACTS

The Offline Software System of the Super Tau-Charm Facility (OSCAR) [32, 33] serves as the offline event processing framework for the STCF. It provides common services for data processing and a suite of application tools dedicated to event generation, simulation, reconstruction, and physics analysis. For simulation purposes, OSCAR incorporates generation of τ-charm physics processes facilitated by the KKMC [34] generator, while particle decays are modeled with EvtGen as used by BESIII experiment [35], both seamlessly integrated within the framework. The STCF detector geometry is described using the Detector Description Toolkit, DD4Hep [36], with all geometric parameters stored in compact files utilizing the eXtensible Markup Language (XML) [37]. To simulate the interaction of particles with the detector comprehensively, Geant4 [38] is integrated into OSCAR, ensuring a sophisticated full simulation. For track reconstruction, the track finding algorithm based on Hough Transform is developed in OSCAR.

The interface between OSCAR and ACTS facilitates the transforming of experimental geometry, measurements, and

initial track estimates into corresponding ACTS representations. Geometry plugins within ACTS are tailored to streamline the conversion of experimental geometry representations, such as DD4hep or TGeo [39], into ACTS internal geometry description. For ITK, the transformation involves converting the signal readout unit tube within each μ-RWELL layer into sensitive cylinder surfaces. Similarly, for MDC, the process entails transforming each sense wire within a drift cell into a line surface. Leveraging dedicated material mapping tools within ACTS, detailed material descriptions are projected onto internal auxiliary surfaces of the ACTS geometry. For the conversion of measurements and initial track parameters, two ROOT [40]-based readers have been developed. One reader extracts simulated hits from full simulation data and converts them into ACTS measurements taking into account the resolution of the detectors. Another reader converts the initial estimate of the track parameters provided by the Hough Transform algorithm into ACTS track parameters.

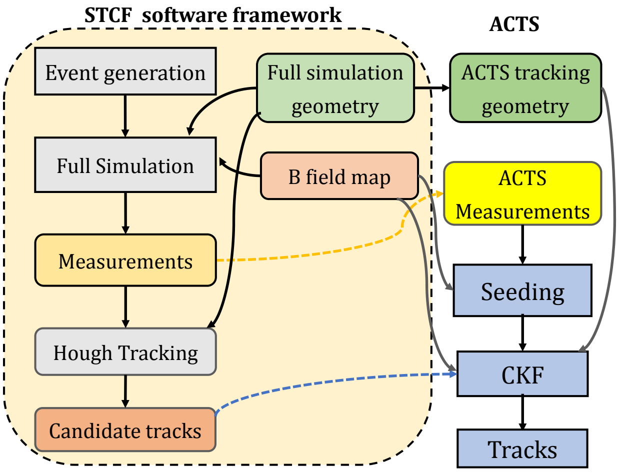

Fig. 2. The workflow of studying tracking performance using STCF software framework and ACTS.

B. ACTS seed finding

The seeding algorithm in ACTS aims to find a few measurements which can provide position coordinates (x, y, z) in the global coordinate frame associated with a single particle to initiate the track following process. Without a seed, a particle cannot be reconstructed, hence the seed finding algorithm aims to find at least one seed for each particle in the detector acceptance region.

In a uniform magnetic field along the global z axis, the helical trajectory of a charged particle is accurately defined by three measurements, thus forming a seed. In the case of STCF, these seeds are generated by combining three compatible measurements from the ITK detector with one measurement per ITK layer, as illustrated in Fig. 3. For each candidate seed, the curvature and center of the circle on the x-y plane are determined using the Conformal Transform [41, 42]. Subsequently, these parameters are utilized to calculate the transverse momentum and the transverse impact parameter on the x-y plane, which are required to satisfy the criteria optimized for the relevant physics processes. The bending of the seed in the r-z plane is also required to be smaller than a threshold, which is optimized taking into account the impact of magnetic field and multiple scattering. See Ref. [43] for a detailed description of the ACTS seeding.

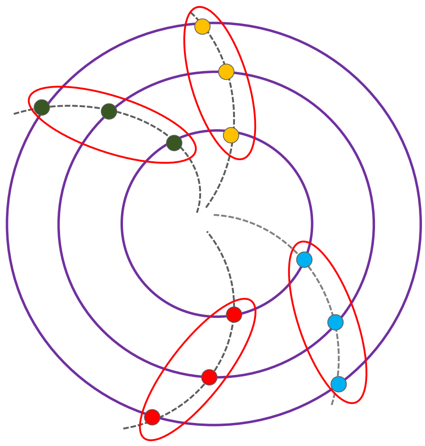

Fig. 3. Illustration of ACTS seeding using measurements from STCF ITK.

C. Track finding with Hough Transform

The principle of Hough Transform for track finding is illustrated in Fig. 4. With the presence of a magnetic field along global z axis, the projection of the track in the geometrical transverse x-y plane is a circle and the projection of the track in the geometrical s-z plane (s is the path length of the track in the x-y plane) is a straight line. The Conformal Transform can convert the projection of a track in the transverse x-y plane passing through the origin into a straight line, with a drift circle tangent to the projection of the track converted to another circle tangent to the straight line, in the Conformal u-v space. For a displaced track which has non-zero but relatively small transverse impact track parameter, i.e. d_0, compared to the radius of the circle projected in the geometrical transverse x-y plane, as shown in Fig. 4 left panel, the trajectory of the transformed measurements (either a point or a drift circle) on the Conformal space can be approximately parameterized using a straight line, as shown in Fig. 4 middle panel. The Hough Transform for track finding operates on the principle that a straight line in the geometrical or Conformal space can be described by two parameters, angle θ of its normal and its algebraic distance ρ from the origin. For a point with coordinate (u, v) on the straight line, it can be transformed into a sinusoidal curve in the Hough space, i.e.

$$\rho = u \cdot cos\alpha + v \cdot sin\alpha \tag{1}$$

, and for a circle with center (u, v) and radius r tangent to the

straight line, it can be transformed into two sinusoidal curves in the Hough space, i.e.

$$\rho = u \cdot cos\alpha + v \cdot sin\alpha \pm r \quad (2)$$

The process of finding the measurements or drift circles that arise from the same track in either the Conformal u-v space or the geometrical s-z space becomes identifying the curves that have an intersection in Hough space as shown in Fig. 4 right panel, i.e. a 2D histogram with optimized binning taking into account the resolution of the track parameters are filled if a curve passes through it and the peaks of the histograms are identified, as detailed in Ref. [20]. The parameters at the intersection can be converted to the track parameters describing the track projected to either the geometrical transverse x-y plane or the geometrical s-z plane.

The workflow of track finding using Hough Transform in OCSCAR is shown in Fig.5. Initially, the measurements from ITK and MDC axial wires are used to reconstruct the projections of the tracks on the x-y plane, denoted as 2D tracks, followed by circle fitting to extract track parameters of the 2D tracks. This is succeeded by associating the MDC stereo wire measurement candidates to the 2D tracks, where the z position and path length s of the track at the stereo wires are derived simultaneously. For each stereo wire measurement, two z position solutions can be obtained, and measurements from other tracks may be wrongly assigned to a 2D track. Therefore, a secondary application of Hough Transform is employed to find the tracks in the s-z plane. More details can be found in Ref. [20].

D. Track finding with ACTS CKF

Starting from a set of initial track parameters, the ACTS CKF is driven by the ACTS track propagator to search for compatible measurements at a particular surface through KF track fitting, as illustrated by Fig. 6. This process is also known as track following. The measurement providing the best fitting quality is associated to the track and used to filter the track parameters for further track propagation.

IV. PERFORMANCE STUDIES

A. Monte-Carlo samples

The J/ψ decay process $J/\psi \to \Lambda(\to p\pi^-)\bar{\Lambda}(\to \bar{p}\pi^+)$ is an important benchmark process at STCF allowing for several important physics studies relevant to Λ. Those signal events generated with the KKMC and EvtGen generators in OSCAR without considering bream-related backgrounds are used to evaluate the tracking performance. The 2D distributions of the cosθ versus p_T, vertex displacement in the x-y plane V_{xy} versus p_T, and transverse impact track parameter d_0 versus p_T, for proton (anti-proton), denoted as $p(\bar{p})$, and π in the $J/\psi \to \Lambda(\to p\pi^-)\bar{\Lambda}(\to \bar{p}\pi^+)$ events are shown in Fig. 7. The π has a low momentum with p_T below 310 MeV/c and $p(\bar{p})$ has a p_T up to 1.1 GeV/c. A non-negligible amount of particles are decaying outside the first layer of ITK. However, most of the tracks have d_0 smaller than the radius of the first ITk layer, in particular for $p(\bar{p})$.

Following event generation, Geant4 simulates hits from final state particles decaying from primary particles interacting with the STCF tracking system in a uniform magnetic field of 1T. Detector measurements are then generated by applying Gaussian smearing to the positions of simulated hits, with zero means and widths corresponding to the detector resolutions.

B. Track finding performance

The performance of track finding, including seed finding using either ACTS seeding algorithm or Hough Transform algorithm at the first stage, and track following using ACTS CKF at the second stage, is studied. Considering the acceptance of STCF tracking system, only truth particles with p_T above 50 MeV and |cosθ| below 0.94 are considered in the performance metrics evaluation, which involves identifying the primary particle [21] of a seed or a track, i.e. the simulated particle which has the most simulated hits contributing to this seed or track.

The seeding process serves as the initial step in track finding using CKF, which should provide seeds for all particles in an ideal case. The ACTS seeding efficiency is defined as the fraction of particles in the tracking system acceptance region that have matched seeds with all three hits arising from the same particle. The seeding efficiency using Hough Transform is defined by requiring that a matched seed has at least 50% hits from its primary particle.

For ACTS seeding, it's only possible to find seeds for a track if the particle produces hits in all three layers of ITK, indicating a vertex displacement below 66.5 mm. The comparison between efficiencies of ACTS seeding and Hough Transform algorithm as a function of V_{xy} of the particles is shown in Fig. 8 top panels. The ACTS seeding efficiency approaches 100% when the number of measurements from ITK is no less than 3. In particular, the ACTS seeding provides better seeding efficiency than Hough Transform for π with small V_{xy}. However, ACTS seeding efficiency immediately drops to zero if the number of measurements from ITK is below 3, indicating a significant limitation of ACTS seeding algorithm, in particular for long-lived particles. The Hough Transform algorithm, functioning as a global tracking algorithm, demonstrates reduced sensitivity to the number of ITK layers particles traverse. Fig. 8 bottom panels shows the seeding efficiency as a function of particle p_T. It is observed that Hough Transform algorithm can provide an efficiency above 90% for $p(\bar{p})$ with p_T above 350 MeV/c and above 80% for π with p_T above 85 MeV/c, which is much improved compared to ACTS seeding.

The reconstructed tracks are required to have at least five measurements on the track and have reconstructed |cosθ| < 0.94. A reconstructed track is matched to its primary particle if the fraction of its hits from its primary particle, i.e. track

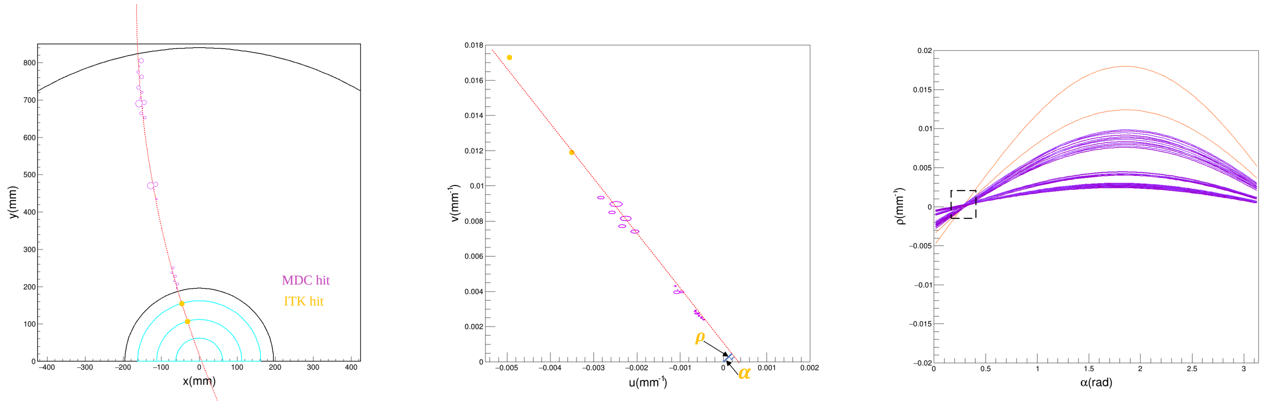

Fig. 4. An example of mapping detector measurements in geometrical transverse x-y plane (left) to the Conformal u-v space (middle) and eventually to the Hough curves in Hough space (right) for the particle p in a $J/\psi \to \Lambda(\to p\pi^-)\bar{\Lambda}(\to \bar{p}\pi^+)$ event. The particle decays between the first and the second layer of the ITK detector and hence has two hits on ITK. The hits or curves for ITK hits and MDC hits are shown by yellow and purple colors, respectively.

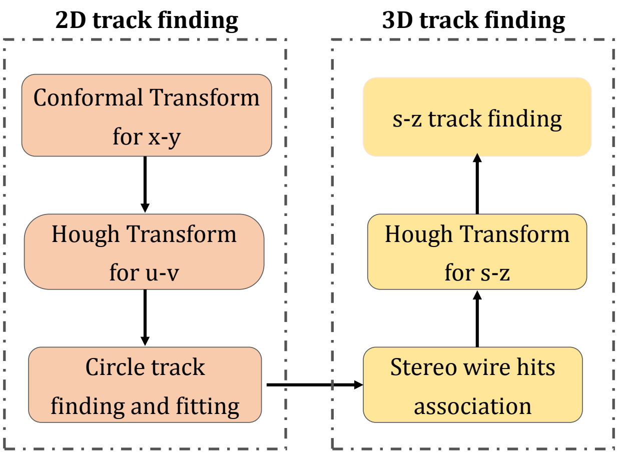

Fig. 5. The workflow of track finding using Hough Transform in OSCAR.

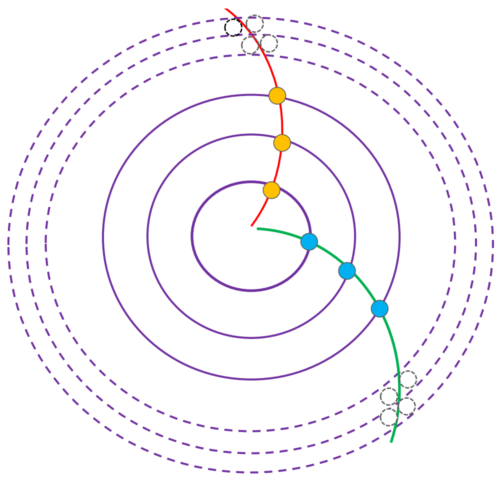

Fig. 6. Illustration of track finding using ACTS CKF with STCF ITK and MDC. Only two MDC layers are shown in the figure.

purity, is no less than 50%, and it's classified as a fake track if it's not matched to its primary particle. If more than one reconstructed tracks are matched to the same simulated particle, the track with the highest track purity is classified as the real track and others are classified as duplicate tracks. The track reconstruction efficiency is defined by the fraction of particles which have matched reconstructed tracks among the particles which have at least 5 simulated hits in the detector acceptance region. The fake rate is defined by the fraction of fake tracks among the reconstructed tracks. The duplicate rate is defined by the fraction of particles which have at least one duplicate track among the particles which have at least 5 simulated hits in the detector acceptance region.

Figure 9 shows the tracking efficiency as a function of particle V_{xy} and p_T. As expected, the tracking efficiency using ACTS seeding and CKF drops to zero when V_{xy} of the particle exceeds 66.5 mm, while the tracking efficiency with Hough Transform and CKF is less dependent on the particle V_{xy}. A tracking efficiency above 80% for $p(\bar{p})$ with p_T above 350 MeV/c and above 70% for π with p_T above 85 MeV/c is achieved using combined Hough Transform and CKF.

Figure 10 shows the fake rate and duplicate rate using the two different seeding strategies. The fake rate is less than 0.4% and a non-negligible amount of duplicate tracks are found for particles with p_T below 150 MeV/c, which have looping trajectories when traversing the detector in a magnetic field. ACTS seeding results in lower fake rate and duplicate rate than that using Hough Transform as seeding.

The track finding performance of the alternative MAPS-based ITK for the long-lived particles is compared to that of the μ-RWELL-based ITK. Figure 11 shows the tracking efficiency, fake rate and duplicate rate of the combined Hough Transform and ACTS CKF for the two different ITK designs. Since the first two layers of the MAPS-based

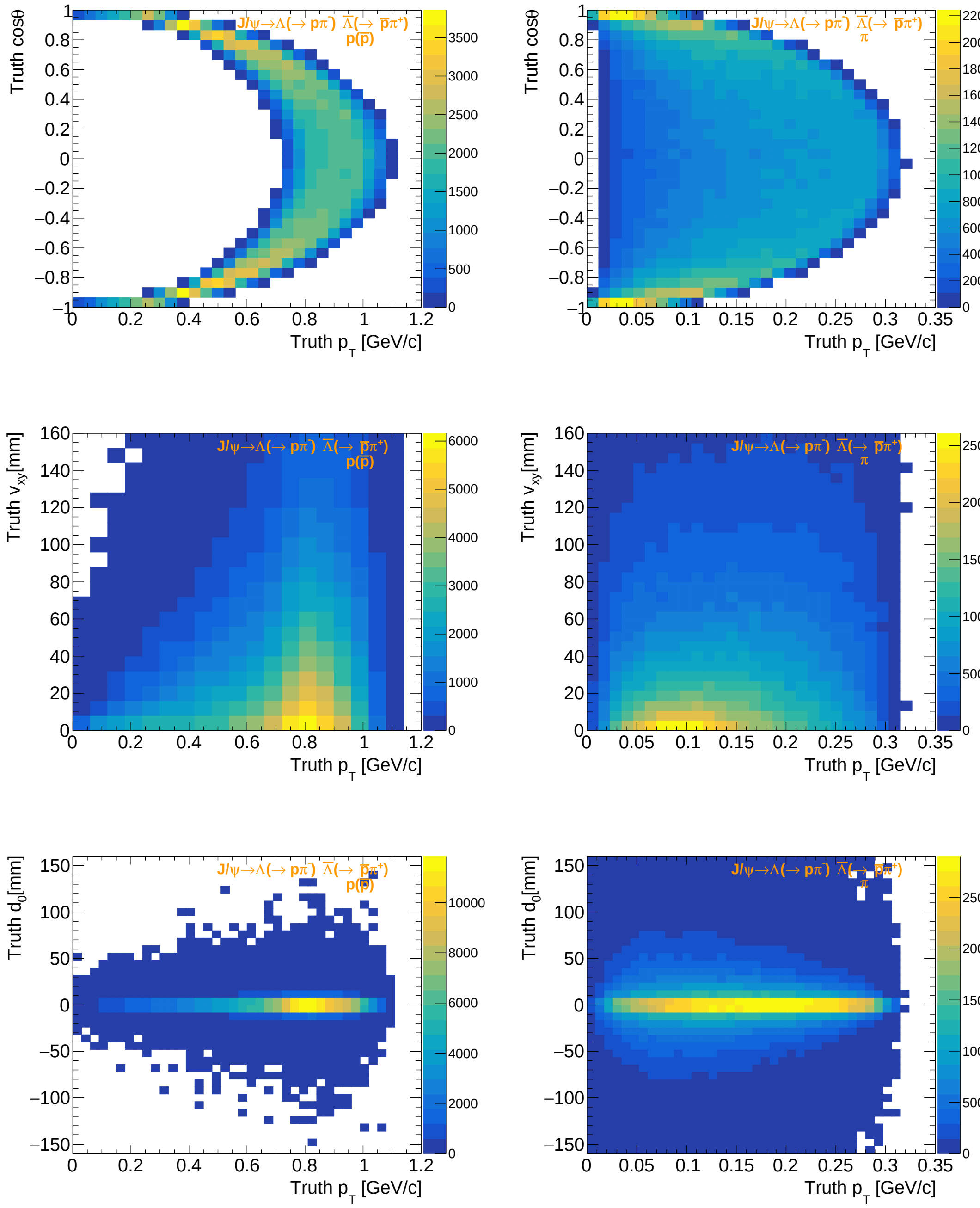

Fig. 7. The distributions of particle cosθ versus p_T (top) and particle vertex displacement in the x-y plane V_{xy} versus p_T (middle), and d_0 versus p_T (bottom) for $p(\bar{p})$ (left) and π (right) in $J/\psi \to \Lambda(\to p\pi^-)\bar{\Lambda}(\to \bar{p}\pi^+)$ events.

ITK have smaller radii than the μ-RWELL-based ITK, the MAPS-based ITK is less robust against the long-lived particles and provides slightly worse tracking efficiency than the μ-RWELL-based ITK. The occurrence of fake and duplicate tracks with the two designs is at similar level.

V. CONCLUSION

Processes with long-lived particles provide opportunities for probing CP, strong interaction etc. at the next generation of Tau-Charm facility, STCF. However, high-performance track reconstruction for long-lived particles is a challenging and complicated task based on the tracking system of STCF. CKF is one of the most commonly used track find-

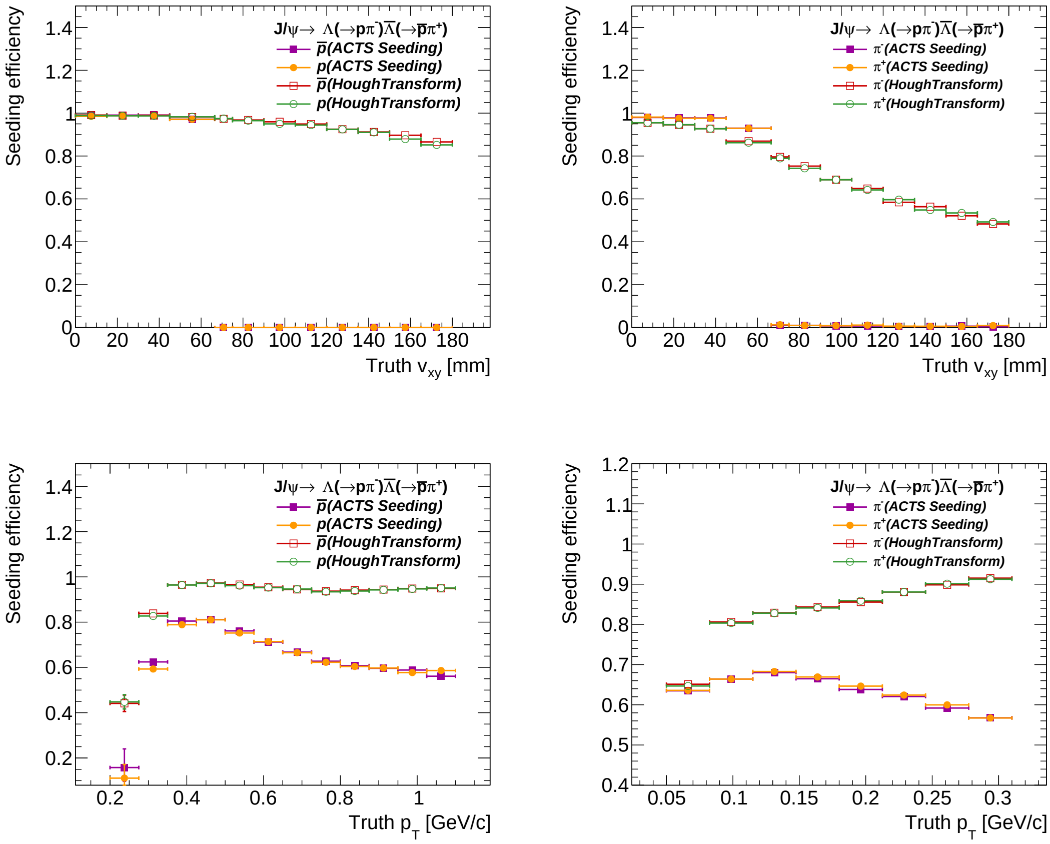

Fig. 8. The seeding efficiency as a function of the particle V_{xy} (top) and p_T (bottom) for $p(\bar{p})$ (left) and $\pi^+(\pi^-)$ (right) in 200k $J/\psi \to \Lambda(\to p\pi^-)\bar{\Lambda}(\to \bar{p}\pi^+)$ events. The solid purple square and yellow dot represent the results of ACTS seeding for particles with negative charge and positive charge, respectively. The hollow red square and green circle represent the results of Hough Transform for particles with negative charge and positive charge, respectively.

ing algorithms at HEP experiments with its performance subject to the performance of the corresponding seeding algorithm. For long-lived particles, CKF using traditional seeding strategy, which often uses measurements from inner detector(s), demonstrates significant performance loss. Based on the STCF offline software and the common tracking software ACTS, the combined performance of using Hough Transform as a seeding algorithm for ACTS CKF has been studied for the first time. The performance was evaluated using $J/\psi \to \Lambda(\to p\pi^-)\bar{\Lambda}(\to \bar{p}\pi^+)$ events at STCF. The study shows that CKF steered by Hough Transform ends up with improved efficiency compared to CKF steered by traditional seeding algorithm for particles with large vertex displacement. The tracking efficiency using combined Hough Transform and CKF is 80% for proton and anti-proton with p_T above 350 MeV/c, and above 70% for π with p_T above 85 MeV/c, with negligible occurrence of fake tracks. Duplicate tracks also exist, mainly arising from particles with p_T below 150 MeV/c with looping trajectories. Future development like extension of the 2D Hough space to 3D Hough space, where a track projection on the x-y plane not passing through origin is described by three dedicated parameters, is foreseen to further enhance the tracking efficiency for long-lived particles at STCF and beyond.

ACKNOWLEDGMENTS

This work is supported in part by the National Natural Science Foundation of China (NSFC) under Contract Nos. 12375194, 12341504, 12375197, 12025502.

[1] M. K. Gaillard, P. D. Grannis, F. J. Sciulli, The standard model of particle physics, Rev. Mod. Phys. 71 (1999) S96–S111. doi:10.1103/RevModPhys.71.S96.

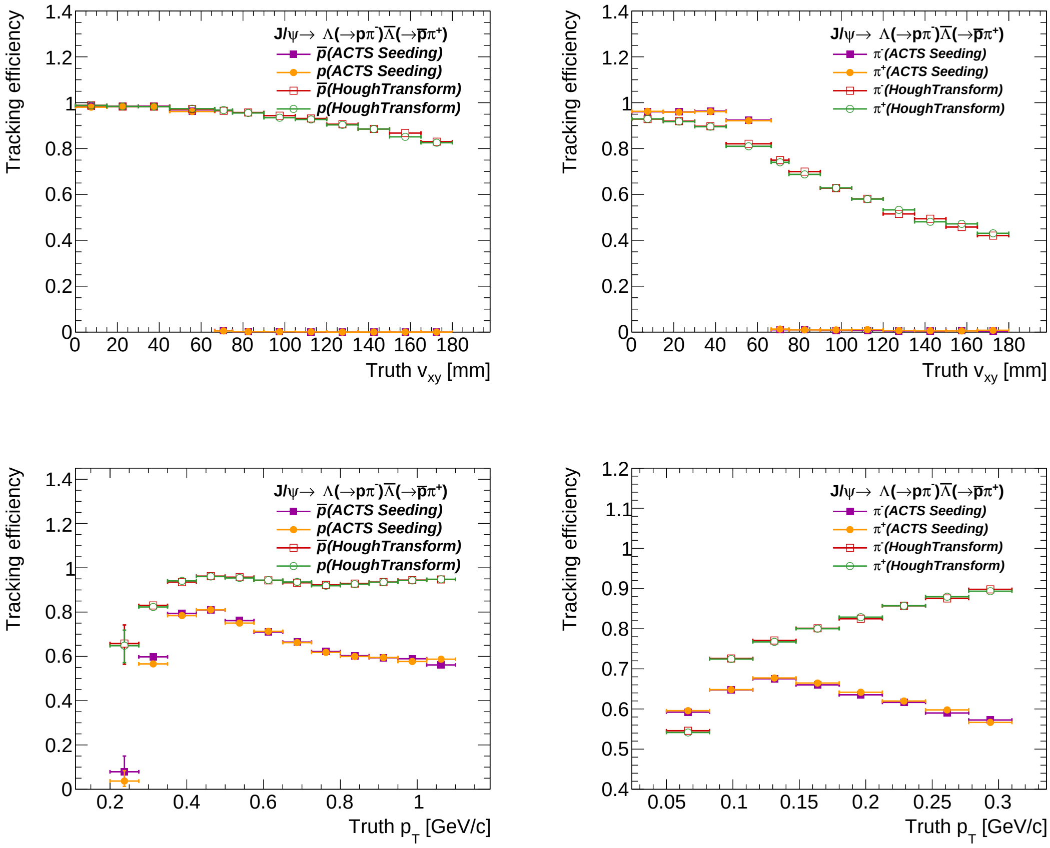

Fig. 9. The tracking efficiency as a function of the particle V_{xy} (top) and p_T (bottom) for $p(\bar{p})$ (left) and $\pi^+(\pi^-)$ (right) in 200k $J/\psi \to \Lambda(\to p\pi^-)\bar{\Lambda}(\to \bar{p}\pi^+)$ events. The solid purple square and yellow dot represent the results with ACTS seeding for particles with negative charge and positive charge, respectively. The hollow red square and green circle represent the results with Hough Transform for particles with negative charge and positive charge, respectively.

[2] J. F. Donoghue, E. Golowich, B. R. Holstein, Dynamics of the Standard Model, 2nd Edition, Cambridge Monographs on Particle Physics, Nuclear Physics and Cosmology, Cambridge University Press, 2014. doi:10.1017/CBO9780511803512.

[3] M. Ablikim, et al., Design and construction of the BESIII detector, Nuclear Instruments and Methods in Physics Research Section A: Accelerators, Spectrometers, Detectors and Associated Equipment 614 (3) (2010) 345–399. doi:10.1016/j.nima.2009.12.050.

[4] H. Peng, Y. Zheng, X. Zhou, Super Tau-Charm Facility of China, PHYSICS 49 (8) (2020) 513–524. doi:10.7693/wl20200803.

[5] M. Achasov, et al., STCF conceptual design report (Volume 1): Physics & detector, Frontiers of Physics 19 (1) (2023) 14701. doi:10.1007/s11467-023-1333-z.

[6] L. Lee, C. Ohm, A. Soffer, T.-T. Yu, Collider searches for long-lived particles beyond the Standard Model, Progress in Particle and Nuclear Physics 106 (2019) 210–255. doi:10.1016/j.ppnp.2019.02.006.

[7] X.-G. He, H. Steger, G. Valencia, Status of CP violation in hyperon decays, Physics Letters B 272 (3) (1991) 411–418. doi:10.1016/0370-2693(91)91851-L.

[8] X.-G. He, CP violation from supersymmetry in hyperon decays, Nuclear Physics A 684 (1) (2001) 710–712, few-Body Problems in Physics. doi:10.1016/S0375-9474(01)00469-9.

[9] BESIII Collaboration, Polarization and entanglement in baryon–antibaryon pair production in electron–positron annihilation, Nature Physics 15 (7) (2019) 631–634. doi:10.1038/s41567-019-0494-8.

[10] R. E. Kalman, A New Approach to Linear Filtering and Prediction Problems, Journal of Basic Engineering 82 (1) (1960) 35–45. doi:10.1115/1.3662552.

[11] N. Braun, Combinatorial Kalman Filter, Springer International Publishing, Cham, 2019, pp. 117–174. doi:10.1007/978-3-030-24997-7_6.

[12] R. Frühwirth, A. Strandlie, Track Finding, Springer International Publishing, Cham, 2021, pp. 81–102. doi:10.1007/978-3-030-65771-0_5.

[13] ATLAS Collaboration, Software Performance of the ATLAS Track Reconstruction for LHC Run 3, Computing and Software for Big Science 8 (1) (2024) 9. doi:10.1007/s41781-023-00111-y.

[14] CMS Collaboration, CMS tracking performance in Run 2 and early Run 3, Tech. rep., CERN, Geneva (2024). arXiv:2312.08017, doi:10.22323/1.448.0074.

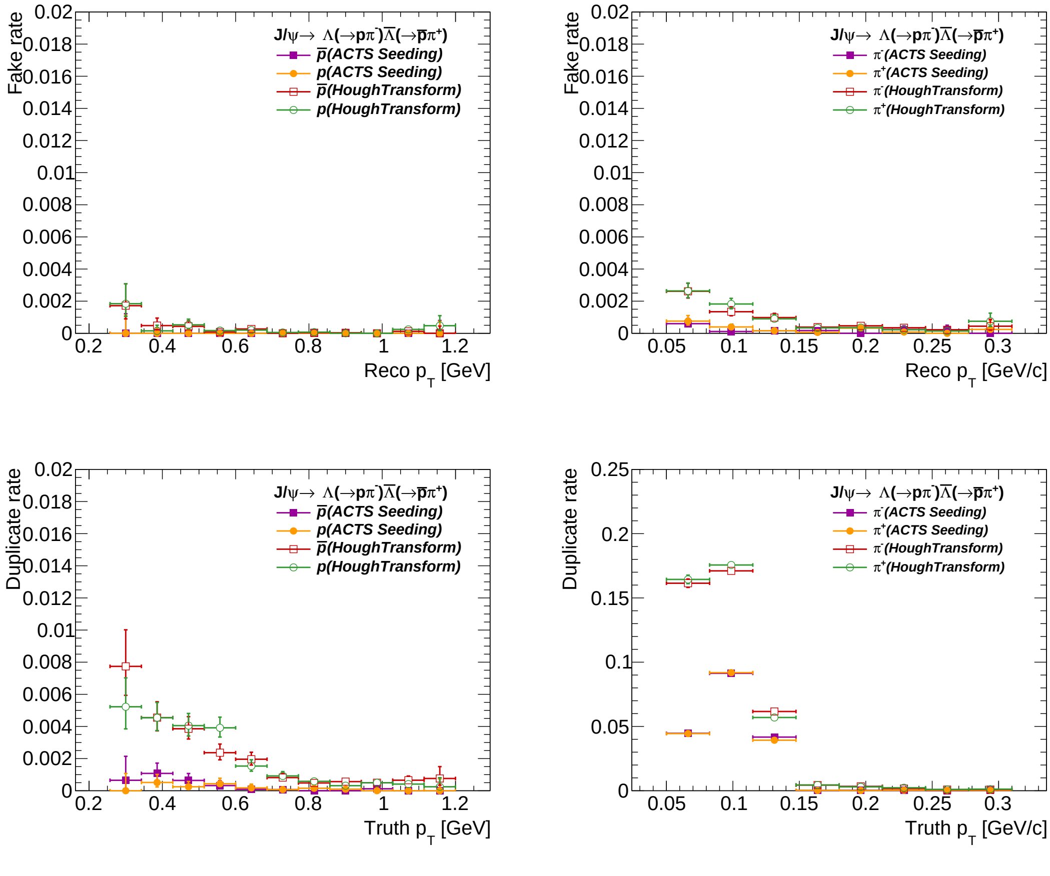

Fig. 10. The fake rate as a function of the track p_T (top) and duplicate rate as a function of the particle p_T (bottom) for $p(\bar{p})$ (left) and $\pi^+(\pi^-)$ (right) in 200k $J/\psi \rightarrow \Lambda(\rightarrow p\pi^-)\bar{\Lambda}(\rightarrow \bar{p}\pi^+)$ events. The solid purple square and yellow dot represent the results with ACTS seeding for particles with negative charge and positive charge, respectively. The hollow red square and green circle represent the results with Hough Transform for particles with negative charge and positive charge, respectively.

[15] V. Bertacchi, et al., Track finding at Belle-II, Computer Physics Communications 259 (2021) 107610. doi:10.1016/j.cpc.2020.107610.

[16] M.-Y. Liu, W.-D. Li, X.-T. Huang, Y. Zhang, T. Lin, Y. Yuan, Simulation and reconstruction of particle trajectories in the CEPC drift chamber, Nuclear Science and Techniques 35 (8) (2024) 128. doi:10.1007/s41365-024-01497-z.

[17] X. Lou, The Circular Electron Positron Collider, Nature Reviews Physics 1 (4) (2019) 232–234. doi:10.1038/s42254-019-0047-1.

[18] S. Pohl, Track reconstruction at the first level trigger of the Belle II experiment (April 2018). doi:10.5282/edoc.22085.

[19] J. Zhang, Y. Zhang, H.-M. Liu, Y. Yuan, X.-Y. Zhang, L.-Y. Dong, Z. Huang, X.-B. Ji, H.-B. Li, W.-G. Li, J.-D. Lu, Y. Nakatsugawa, L.-L. Wang, M. Wang, L.-H. Wu, Low transverse momentum track reconstruction based on the Hough transform for the BESIII drift chamber, Radiation Detection Technology and Methods 2 (1) (2018) 20. doi:10.1007/s41605-018-0052-4.

[20] H. Zhou, K. Sun, Z. Lu, H. Li, X. Ai, J. Zhang, X. Huang, J. Liu, Global track finding based on the Hough transform in the STCF detector, Nuclear Instruments and Methods in Physics Research Section A: Accelerators, Spectrometers, Detectors and Associated Equipment 1075 (2025) 170357. doi:10.1016/j.nima.2025.170357.

[21] X. Ai, C. Allaire, N. Calace, A. Czirkos, D. Rousseau, A Common Tracking Software Project (2021). doi:10.1007/s41781-021-00078-8.

[22] A. Salzburger, et al., acts-project/acts: v38.2.0 (Dec. 2024). doi:10.5281/zenodo.14502803.

[23] J. Liu, H. Pang, C. Wang, X. Ai, X. Chen, Z. Hu, FASER experiment: An introduction and research progress, Chinese Science Bulletin 69 (8) (2024) 1025–1033. doi:10.1360/TB-2023-1034.

[24] J. D. Osborn, A. D. Frawley, J. Huang, S. Lee, H. P. D. Costa, M. Peters, C. Pinkenburg, C. Roland, H. Yu, Implementation of ACTS into sPHENIX track reconstruction, Computing and Software for Big Science 5 (1) (2021). doi:10.1007/978-3-030-24997-7_6.

[25] X. Ai, X. Huang, Y. Liu, Implementation of ACTS for STCF track reconstruction, Journal of Instrumentation 18 (07) (2023) P07026. doi:10.1088/1748-0221/18/07/P07026.

[26] Y. Liu, X.-C. Ai, G.-Y. Xiao, Y.-X. Li, L.-H. Wu, L.-L. Wang, J.-N. Dong, M.-Y. Dong, Q.-L. Geng, M. Luo, Y. Niu, A.-Q. Wang, C.-X. Wang, M. Wang, L. Zhang, L. Zhang, R.-K. Zhang, Y. Zhang, M.-G. Zhao, Y. Zhou, Simulation study of BESIII with stitched CMOS pixel detector using ACTS,

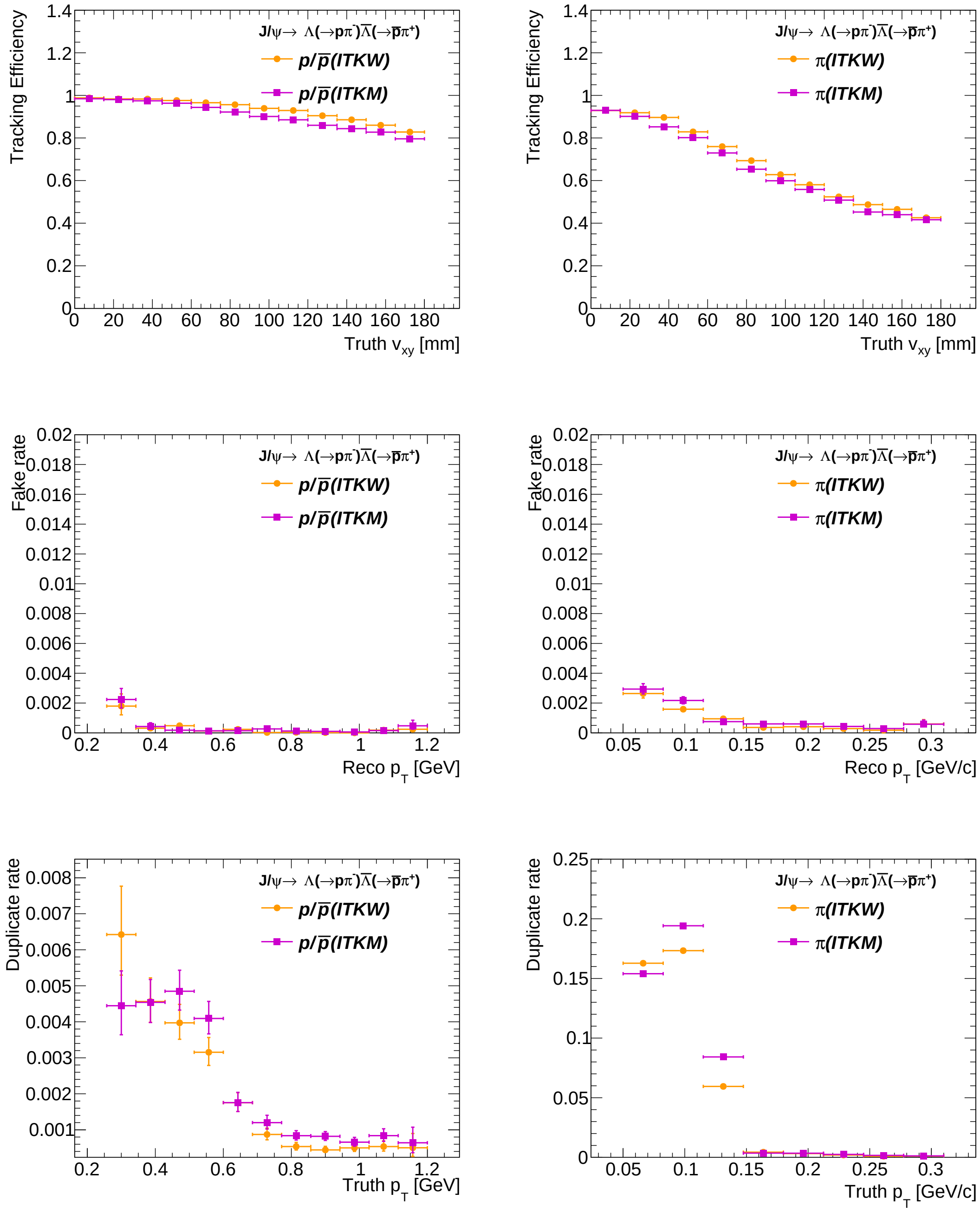

Fig. 11. The tracking efficiency as a function of the particle V_{xy} (top), fake rate as a function of the track p_T (middle) and duplicate rate as a function of the particle p_T (bottom) for $p(\bar{p})$ (left) and π (right) in 200k $J/\psi \to \Lambda(\to p\pi^-)\bar{\Lambda}(\to \bar{p}\pi^+)$ events using combined Hough Transform and ACTS CKF. The yellow dot and purple square represent the results with the μ-RWELL-based ITK (denoted as ITKW) and MAPS-based ITK (denoted as ITKM), respectively.

Nuclear Science and Techniques 34 (12) (2023) 203. doi:10.1007/s41365-023-01353-6.

[27] X. Ai, X. Huang, H. Li, W. Li, T. Lin, Y. Liu, L. Wu, Application of ACTS for gaseous tracking detectors, Modern Physics Letters A 0 (0) (0) 2440009. doi:10.1142/S0217732324400091.

[28] Y. Zhou, Y. Lv, L. Shang, D. Hong, G. Song, J. Liu, J. Feng, M. Shao, X. Wang, Z. Zhang, Fabrication and performance of a μRWELL detector with Diamond-Like Carbon resistive electrode and two-dimensional readout, Nuclear Instruments and Methods in Physics Research Section A: Accelerators, Spectrometers, Detectors and Associated Equipment 927 (2019) 31–36. doi:https://doi.org/10.1016/j.nima.

2019.01.036.

[29] P. Li, S. Chen, Q. Liu, Z. Zhang, A. Wang, J. Feng, B. Hou, H. Liu, L. Zhao, M. Shao, J. Liu, Y. Zheng, Study of hybrid micropattern gaseous detector with CsI photocathode for Super Tau-Charm facility RICH, Journal of Instrumentation 18 (04) (2023) P04028. doi:10.1088/1748-0221/18/04/P04028.

[30] B. Qi, M. Shao, J. Liu, Imaging-based likelihood analysis for the STCF DTOF detector, Nuclear Instruments and Methods in Physics Research Section A: Accelerators, Spectrometers, Detectors and Associated Equipment 1049 (2023) 168090. doi:https://doi.org/10.1016/j.nima.2023.168090.

[31] Z. Jia, H. Yu, H. Mo, Y. Song, Z. Shen, Y. Zhang, J. Liu, H. Peng, A light yield enhancement method using wavelength shifter for the STCF EMC, Nuclear Instruments and Methods in Physics Research Section A: Accelerators, Spectrometers, Detectors and Associated Equipment 1050 (2023) 168173. doi:https://doi.org/10.1016/j.nima.2023.168173.

[32] W. Huang, H. Li, H. Zhou, T. Li, Q. Li, X. Huang, Design and development of the core software for STCF offline data processing, Journal of Instrumentation 18 (03) (2023) P03004. doi:10.1088/1748-0221/18/03/p03004.

[33] X. Ai, X. Huang, T. Li, B. Qi, X. Qin, Design and development of STCF offline software, Modern Physics Letters A 0 (0) (0) 2440006. doi:10.1142/S0217732324400066.

[34] S. Jadach, B. F. L. Ward, Z. Wąs, Coherent exclusive exponentiation for precision Monte Carlo calculations, Phys. Rev. D 63 (2001) 113009. doi:10.1103/PhysRevD.63.113009.

[35] P. Rong-Gang, Event generators at BESIII, Chinese Physics C 32 (8) (2008) 599. doi:10.1088/1674-1137/32/8/001.

[36] M. Frank, F. Gaede, C. Grefe, P. Mato, DD4hep: A Detector Description Toolkit for High Energy Physics Experiments, Journal of Physics: Conference Series 513 (2) (2014) 022010. doi:10.1088/1742-6596/513/2/022010.

[37] T. Bray, J. Paoli, C. M. Sperberg-Mcqueen, Extensible markup language, World Wide Web Journal 2 (4) (1997) 29–66. doi:10.1007/978-1-4302-0187-8_6.

[38] S. Agostinelli, et al., Geant4—a simulation toolkit, Nuclear Instruments and Methods in Physics Research Section A: Accelerators, Spectrometers, Detectors and Associated Equipment 506 (3) (2003) 250–303. doi:10.1016/S0168-9002(03)01368-8.

[39] R. Brun, A. Gheata, M. Gheata, The ROOT geometry package, Nuclear Instruments and Methods in Physics Research Section A: Accelerators, Spectrometers, Detectors and Associated Equipment 502 (2) (2003) 676–680, proceedings of the VIII International Workshop on Advanced Computing and Analysis Techniques in Physics Research. doi:10.1016/S0168-9002(03)00541-2.

[40] R. Brun, F. Rademakers, ROOT — An object oriented data analysis framework, Nuclear Instruments and Methods in Physics Research Section A: Accelerators, Spectrometers, Detectors and Associated Equipment 389 (1) (1997) 81–86, new Computing Techniques in Physics Research V. doi:10.1016/S0168-9002(97)00048-X.

[41] M. Hansroul, H. Jeremie, D. Savard, Fast circle fit with the conformal mapping method, Nuclear Instruments and Methods in Physics Research Section A: Accelerators, Spectrometers, Detectors and Associated Equipment 270 (2) (1988) 498–501. doi:10.1016/0168-9002(88)90722-X.

[42] L. Qiu-Guang, Z. Shi-Lei, L. Wei-Guo, et al., Track construction using the TSF method for the BESIII main drift chamber, Chinese Physics C 32 (7) (2008) 565–571. doi:10.1088/1674-1137/32/7/011.

[43] ACTS Seeding, https://acts.readthedocs.io/en/latest/core/reconstruction/pattern_recognition/seeding.html.